Smart Structures and Systems, *Vol. 26, No. 6 (2020) 809-817*
DOI: https://doi.org/10.12989/sss.2020.26.6.809

Analysis of nonlocal Kelvin's model for embedded microtubules: Via viscoelastic medium

Muhammad Taj[1], Mohamed A. Khadimallah[2,3*], Muzamal Hussain[4], Khaled Mohamed Khedher[5,6], Raja A. Shamim[1], Manzoor Ahmad[1] and Abdelouahed Tounsi[7]

[1]*Department of Mathematics, University of Azad Jammu and Kashmir, Muzaffarabad, 1300, Azad Kashmir, Pakistan*
[2]*Prince Sattam Bin Abdulaziz University, College of Engineering, Civil Engineering Department, BP 655, Al-Kharj, 16273, Saudi Arabia*
[3]*Laboratory of Systems and Applied Mechanics, Polytechnic School of Tunisia, University of Carthage, Tunis, Tunisia*
[4]*Department of Mathematics, Govt. College University Faisalabad, 38000, Faisalabad, Pakistan*
[5]*Department of Civil Engineering, College of Engineering, King Khalid University, Abha 61421, Saudi Arabia*
[6]*Department of Civil Engineering, High Institute of Technological Studies, Mrezgua University Campus, Nabeul 8000, Tunisia*
[7]*YFL (Yonsei Frontier Lab), Yonsei University, Seoul, Korea*

(*Received June 9, 2020, Revised October 13, 2020, Accepted October 27, 2020*)

Abstract. In cells, the microtubules are surrounded by viscoelastic medium. Microtubules, though very small in size, perform a vital role in transportation of protein and in maintaining the cell shape. During performing these functions waves propagate and this propagation of waves has been investigated using nonlocal elastic theory. But the effect of surrounding medium was not taken into account. To fill this gap, this study considers the viscoelastic medium along with nonlocal elastic theory. The analytical formulas of the velocity of waves, and the results reveal that the presence of medium reduces the velocity. The axisymmetric and nonaxisymmetric waves are separately discussed. Furthermore, the results are compared with the results gained from the studies of free microtubules. The presence of medium around microtubules results in the increase of the flexural rigidity causing a significant decrease in radial wave velocity as compared to axial and circumferential wave velocities. The effect of viscoelastic medium is more obvious on radial wave velocity, to a lesser extent on torsional wave velocity and least on longitudinal wave velocity.

Keywords: microtubules; wave propagation; Kelvin model; viscoelastic medium

1. Introduction

The cytoskeleton of all types of cells comprises of three protein components, intermediate filaments, actin filaments and microtubules (MTs) (Gao and An 2010). Among these, MTs are the stiffest biopolymer which give shape and support to the cell, maintain the strength of the cell and help in cellular movement and deformation (Qian *et al*. 2007). Within the cell, they work like railway tracks in the transportation of secretory vesicles, motor proteins, pigment granules and ions, etc. (Wang *et al*. 2006). They help in distribution of cytoskeletal proteins and organelles to daughter cells during meiosis and mitosis. Structurally, MTs are of hollow cylindrical structure with 30 nm outer diameter and 20 nm inner diameter while length varies from a few nm to 100 μm (De Pablo *et al*. 2003). MTs are composed up of 13 parallel protofilaments joined in the shape of circle (Nogales 2001). These filaments are composed of *αβ*-tubulin dimmers (Gittes *et al*. 1993, Ishida *et al*. 2007). In performing various functions such as in motion of cilia and flagella, in transport of organelle and macromolecule, due to thermal effects and in catastrophic action of MTs, they vibrate and waves are produced along them within the cells (Daneshmand *et al*. 2011). Qian *et al*. (2007) applied the classical elastic shell model for MTs to describe waves and obtained their velocity, and after that same classical model was extended including transverse shear deformations (Daneshmand *et al*. 2011). This model has been used to investigate many other mechanical properties of MTs (Li *et al*. 2006, Taj and Zhang 2011, 2012). In above mentioned studies, orthotropic elastic shell model was used because experimental methods have shown that the bonds along longitudinal direction are much stronger than the bonds along lateral direction in MTs. The bonds along lateral direction between neighboring protofilaments of MTs are considerably weaker than bonds along longitudinal direction of protofilaments (Needleman *et al*. 2005). The elastic moduli along longitudinal and circumferential direction differ remarkably. Along longitudinal direction the elastic modulus is also greater in magnitude than the shear modulus (De Pablo *et al*. 2003). Moreover, along longitudinal direction MTs have shear modulus lesser than elastic modulus (Kasas *et al*. 2004) and along circumferential direction elastic modulus is lower than the elastic modulus along longitudinal direction (Tuszyński *et al*. 2005). Latterly, in Taj and Zhang (2014), the same model is used to study the wave propagation taking into account the surrounding elastic medium. In another study, the viscoelastic effects of the medium were also studied using Kelvin model for the medium

*Corresponding author, Assistant Professor,
E-mail: am.khadimallah@gmail.com; mohamedamine.khadimallah@fsgf.rnu.tn

http://www.techno-press.org/?journal=sss&subpage=7
ISSN: 1738-1584 (Print), 1738-1991 (Online)

surrounding MTs but for the MTs the same classical orthotropic elastic shell model was used (Safeer *et al*. 2019). Also, an orthotropic Pasternak model has been developed to study wave propagation of MTs surrounded by elastic medium (Taj and Zhang 2012). But as MTs are very small structures having effective radius of 12.8 nm and length of a few hundred nanometers. Due to this minute size, small scale effects become more significant. So, the propagating waves are also smaller in wavelength and hence the wave-vector is very large and waves are dispersive. Therefore, small scale effects may be included to describe the mechanics of MTs rather than the classical model (Born and Huang 1954). The lattice dynamics theory changes to nonlocal elastic theory by utilizing interpolation functions (Eringen 1977). The existence of long range interactions in materials is the basic reason of application of nonlocal theory. These forces include van der Waals force, Coulomb force etc. The stiffness of MTs directly depends on the persistence length of MTs and the small scale effects result in the change of the persistence length of MTs (Gao and An 2010, An and Gao 2010, Gao and Lei 2009).

In the past, research on embedded microtubules within viscoelastic medium is rarely done. A limited number of researchers performed analysis first time to investigate the nonlocal behaviour of embedded microtubules (Born and Huang 1954, Qian *et al.* 2007, De Pablo *et al*. 2003, Nogales 2001). So far as reviewed from the literature, nonlocal orthotropic Kelvin like model for wave propagation along embedded microtubules within viscoelastic medium has not been investigated, wave velocity at micro level using different techniques, for example, shear deformation theory (Arefi *et al*. 2018, Lei and Zhang 2018), structural mechanics approach (Moradi-Dastjerdi and Payganeh 2017, Shafiei and Setoodeh 2017), wave propagation (Hussain *et al*. 2019, Hussain and Naeem 2019a), Galerkin method (Do *et al*. 2019, Hussain and Naeem 2019b), nonlocal continuum models (She *et al*. 2019), 3D HSDT (Boutaleb *et al*. 2019), orthotropic Pasternak model (Taj and Zhang 2012), classical elastic shell model for MTs (Qian *et al*. 2007) and small scale effects for MTs (Gao and An 2010, An and Gao 2010, Gao and Lei 2009). Recently, some researcher used different methods for nonlinear modeling (Tohidi *et al*. 2018, Arefi and Zenkour 2017, Arani *et al*. 2016, Krommer *et al*. 2016, Yeh 2016) and for other structures (Boussoula *et al*. 2020, AlSaleh and Fuggini 2020, Lee *et al*. 2019, Zahrai and Kakouei 2019, Poplawski *et al*. 2019).

Applying nonlocal theory, a remarkable change of bending, buckling and post buckling behavior is observed (Gao and An 2010, An and Gao 2010, Shen 2010a, b, Civalek and Demir 2011, Civalek *et al*. 2010). Also, the small scale effects change the vibrational behavior of MTs (Shen 2011). Nonlocal elastic shell model has been applied for the studies relating wave propagation in carbon nanotubes (Wang and Varadan 2007), which have a similar structure like MTs. In Wang and Gao (2016), nonlocal orthotropic elastic shell model was used to investigate the wave velocities for free MTs. They found that when wavelength is smaller than 80 nm, the small scale effects are more important. They used free MTs for such studies but when MTs are embedded in elastic medium, the radial velocity increases considerably (Safeer *et al*. 2019, Taj and Zhang 2014). Motivated by above findings, we combined nonlocal orthotropic elastic shell model with Kelvin model to study the wave phenomenon considering the effects of viscoelastic medium. The analytical formulas of the velocity of waves, and the results reveal that the presence of medium reduces the velocity. The axisymmetric and non-axisymmetric waves are separately discussed. Furthermore, the results are compared with the results gained from the studies of free microtubules. The presence of medium around microtubules results in the increase of the flexural rigidity causing a significant decrease in radial wave velocity as compared to axial and circumferential wave velocities.

2. Materials and methods

We will apply nonlocal orthotropic elastic shell model to analyze the wave propagation of MTs. Surrounding medium of MTs will be modeled by Kelvin model. We will develop nonlocal orthotropic Kelvin-like model by the combination of these models. We will use wave propagation approach to find the wave dispersion relations for MTs in viscoelastic medium.

2.1 Nonlocal orthotropic Kelvin-like model

Cemal Eringen are pioneers of the nonlocal theory (Kröner 1967, Eringen 1972). For an elastic and homogeneous material the stress strain relationships are given below

$$\sigma_{ij,j} = 0 \tag{1}$$

$$\sigma_{ij}(x) = \int \varphi(|x' - x|, \psi) C_{ijkl} \varepsilon_{kl}(x') dV(x') \quad \forall x \in V \tag{2}$$

$$\varepsilon_{ij} = \frac{1}{2}\left(u_{i,j} + u_{j,i}\right) \tag{3}$$

where j denotes the derivative with respect to j, σ_{ij} and ε_{kl} are strain tensor and stress tensor respectively, and elastic modulus tensor is denoted by C_{ijkl}, u_i represents the displacements, the attenuation function is $\varphi(|x' - x|, \tau)$, and $|x' - x|$ denotes the usual distance. Also, $\psi = e_0 a/l$, where e_0 is a material constant, internal characteristics length is represented by a and l denotes the external characteristics length.

The differential form of Eq. (2) is used as nonlocal constitutive relation (Eringen 2002)

$$(1 - (e_o a)^2 \nabla^2)\sigma_{ij} = C_{ijkl}\varepsilon_{kl} \tag{4}$$

where a is the internal characteristic length.

In our studies we have taken $e_0 a$ as a single parameter, known as small scale parameter which represents the effect of size for the nano and micro structures, and ∇^2 is the

Laplace operator. MTs are circular cylindrical pipe having bridge thickness of 1.1 nm, equivalent thickness h is about 2.7 nm, and the effective thickness h_o for bending is about 1.6 nm (Gao and An 2010, Qian *et al*. 2007). Our coordinate system x, y and z are axial, circumferential and radial coordinates respectively whose dimensionless coordinates are $\alpha = x/R$, $\beta = y/R$ and $\gamma = z/R$.

Along α, β and γ directions, the displacement of middle surface are u, v and w, respectively. The geometrical relations are given by Flugge's shell theory (Flugge 1973, Zou and Foster 1995, Paliwal *et al*. 1995)

$$\varepsilon_\alpha = \frac{1}{R}\left(\frac{\partial u}{\partial \alpha} - \gamma \frac{\partial^2 w}{\partial \alpha^2}\right) \tag{5}$$

$$\varepsilon_\beta = \frac{1}{R}\left(\frac{\partial v}{\partial \beta} + w\right) - \frac{\gamma}{R(1+\gamma)}\left(\frac{\partial^2 w}{\partial \beta^2} + w\right) \tag{6}$$

$$\varepsilon_{\alpha\beta} = \frac{\gamma}{R(1+\gamma)}\left[\frac{\partial u}{\partial \beta} + \frac{\partial v}{\partial \alpha} + 2\gamma\left(\frac{\partial v}{\partial \alpha} - \frac{\partial^2 w}{\partial \alpha \partial \beta}\right) + \gamma^2\left(\frac{\partial v}{\partial \alpha} - \frac{\partial^2 w}{\partial \alpha \partial \beta}\right)\right] \tag{7}$$

The stress-strain relationships in dimensionless co-ordinates derived from Eq. (4) is as under Gao and An (2010)

$$\sigma_\alpha - (e_o a)^2 \nabla^2 \sigma_\alpha = E_1(\varepsilon_\alpha + \mu_1 \varepsilon_\beta)/(1-\mu_1\mu_2) \tag{8}$$

$$\sigma_\beta - (e_o a)^2 \nabla^2 \sigma_\beta = E_2(\varepsilon_\beta + \mu_2 \varepsilon_\alpha)/(1-\mu_1\mu_2) \tag{9}$$

$$\tau_{\alpha\beta} - (e_o a)^2 \nabla^2 \tau_{\alpha\beta} = G\varepsilon_{\alpha\beta} \tag{10}$$

where σ_α, σ_β and $\tau_{\alpha\beta}$ are normal and shear stresses, and ε_α, ε_β and $\varepsilon_{\alpha\beta}$ are respective strains; E_1 and E_2 are moduli of elasticity; Poisson's ratios in the directions of α and β are μ_2 and μ_1 respectively. G is modulus of rigidity or shear modulus. Also we have $E_1\mu_1 = E_2\mu_2$ and $\nabla^2 = (\partial^2/\partial\alpha^2 + \partial^2/\partial\beta^2)/R^2$ which is the Laplace operator in dimensionless coordinates. The element of shell in our coordinates is shown in Fig. 1, where (N, S, Q) are the stress resultants and (M) is the moment. The thermal expansion causes pre-stress, which is neglected because the present temperature is considered as the reference temperature. We arrive at the dynamic equilibrium equations

$$\begin{cases} \dfrac{\partial N_\alpha}{\partial \alpha} + \dfrac{\partial S_\beta}{\partial \beta} + \kappa = \rho h R \dfrac{\partial^2 u}{\partial t^2} \\ \dfrac{\partial N_\beta}{\partial \beta} + \dfrac{\partial S_\alpha}{\partial \alpha} + Q_\beta = \rho h R \dfrac{\partial^2 v}{\partial t^2} \\ \dfrac{\partial Q_\alpha}{\partial \alpha} + \dfrac{\partial Q_\beta}{\partial \beta} + N_\beta = \rho h R \dfrac{\partial^2 w}{\partial t^2} \end{cases} \tag{11}$$

$$\begin{cases} \dfrac{\partial M_{\alpha\beta}}{\partial \alpha} + \dfrac{\partial M_\beta}{\partial \beta} - RQ_\beta = 0 \\ \dfrac{\partial M_{\beta\alpha}}{\partial \beta} + \dfrac{\partial M_\alpha}{\partial \alpha} - RQ_\alpha = 0 \end{cases} \tag{12}$$

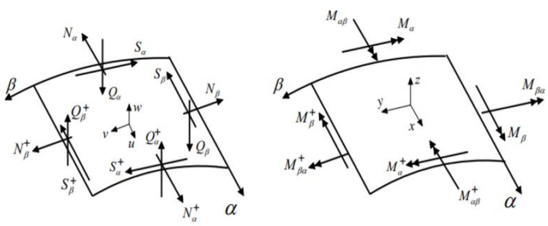

Fig. 1 Resolution of components of stress and moments of the middle surface of MTs

where ρ is the mass density.

The resultants (N, S, Q) are derived from above set of integral equations using the stress components.

$$(1-(e_0 a)^2\nabla^2)\begin{bmatrix} N_\alpha, S_\alpha, \\ M_\alpha, M_{\alpha\beta} \end{bmatrix} = \int_{-\frac{h}{2}}^{\frac{h}{2}} \begin{bmatrix} \sigma_\alpha, \tau_{\alpha\beta}, \\ z\,\sigma_\alpha, z\,\tau_{\alpha\beta} \end{bmatrix}\left(1+\frac{z}{R}\right) dz \tag{13}$$

$$(1-(e_0 a)^2\nabla^2)\begin{bmatrix} N_\beta, S_\beta, \\ M_\beta, M_{\beta\alpha} \end{bmatrix} = \int_{-\frac{h}{2}}^{\frac{h}{2}} \begin{bmatrix} \sigma_\beta, \tau_{\beta\alpha}, \\ z\,\sigma_\beta, z\,\tau_{\beta\alpha} \end{bmatrix} dz \tag{14}$$

$$(1-(e_0 a)^2\nabla^2)(Q_\alpha, Q_\beta) = \int_{-\frac{h}{2}}^{\frac{h}{2}} [\tau_{\alpha z}, \tau_{\beta z}]\, dz \tag{15}$$

where h is thickness of the shell. Above equations result in

$$N_\alpha - (e_o a)^2\nabla^2 N_\alpha = \frac{K}{R}\left[\frac{\partial u}{\partial \alpha} + \mu_1\left(\frac{\partial v}{\partial \beta} + w\right) - c^2\frac{\partial^2 w}{\partial \alpha^2}\right] \tag{16}$$

$$N_\beta - (e_o a)^2\nabla^2 N_\beta = \frac{Kk_1}{R}\left[\frac{\partial v}{\partial \beta} + \mu_2\frac{\partial u}{\partial \alpha} + w + c^2\left(\frac{\partial^2 w}{\partial \beta^2} + w\right)\right] \tag{17}$$

$$S_\alpha - (e_o a)^2\nabla^2 S_\alpha = \frac{Kk_2}{R}\left[\frac{\partial u}{\partial \beta} + \frac{\partial v}{\partial \alpha} - c^2\left(\frac{\partial^2 w}{\partial \alpha \partial \beta} - \frac{\partial v}{\partial \alpha}\right)\right] \tag{18}$$

$$S_\beta - (e_o a)^2\nabla^2 S_\beta = \frac{Kk_2}{R}\left[\frac{\partial u}{\partial \beta} + \frac{\partial v}{\partial \alpha} + c^2\left(\frac{\partial^2 w}{\partial \alpha \partial \beta} + \frac{\partial v}{\partial \alpha}\right)\right] \tag{19}$$

$$M_\alpha - (e_o a)^2\nabla^2 M_\alpha = -Kc^2\left[\frac{\partial u}{\partial \alpha} + \mu_1\frac{\partial v}{\partial \beta} - \left(\frac{\partial^2 w}{\partial \alpha^2} + \mu_1\frac{\partial^2 w}{\partial \beta^2}\right)\right] \tag{20}$$

$$M_\beta - (e_o a)^2\nabla^2 M_\beta = Kk_1c^2\left(\frac{\partial^2 w}{\partial \beta^2} + w + \mu_2\frac{\partial^2 w}{\partial \alpha^2}\right) \tag{21}$$

$$M_{\alpha\beta} - (e_o a)^2\nabla^2 M_{\alpha\beta} = 2Kk_2c^2\left(\frac{\partial v}{\partial \alpha} - \frac{\partial^2 w}{\partial \alpha \partial \beta}\right) \tag{22}$$

$$M_{\beta\alpha} - (e_o a)^2\nabla^2 M_{\beta\alpha} = Kk_2c^2\left(\frac{\partial u}{\partial \beta} - \frac{\partial v}{\partial \alpha} + 2\frac{\partial^2 w}{\partial \alpha \partial \beta}\right) \tag{23}$$

$$Q_\alpha - (e_o a)^2\nabla^2 Q_\alpha = \frac{Kc^2}{R}\left[\frac{\partial^2 u}{\partial \alpha^2} - k_2\frac{\partial^2 u}{\partial \beta^2} + (k_2+\mu_1)\frac{\partial^2 v}{\partial \alpha \partial \beta} - \frac{\partial^3 w}{\partial \alpha^3} - (2k_2+\mu_1)\frac{\partial^3 w}{\partial \alpha \partial \beta^2}\right] \tag{24}$$

$$Q_\beta - (e_o a)^2\nabla^2 Q_\beta = \frac{Kk_1c^2}{R}\begin{bmatrix} 2\frac{k_2}{k_1}\frac{\partial^2 v}{\partial\alpha^2} - \frac{\partial^3 w}{\partial\beta^3} - \\ \frac{\partial w}{\partial\beta} - \left(2\frac{k_2}{k_1} + \mu_2\right)\frac{\partial^3 w}{\partial\alpha^2\partial\beta}\end{bmatrix} \tag{25}$$

where $K = E_1 h/(1-\mu_1\mu_2)$, $k_1 = E_2/E_1$, $k_2 = G(1-\mu_1\mu_2)/E_1$, $c^2 = h_o^3/(12R^2 h)$.

Using Kelvin model for viscoelastic medium and Eqs. (11) and (12) we get Kelvin-like nonlocal orthotropic elastic shell model.

The obtained model is as follows

$$\left[\frac{\partial^2}{\partial\alpha^2} + k_2(1+c^2)\frac{\partial^2}{\partial\beta^2}\right]u + \left[(\mu_1+k_2)\frac{\partial^2}{\partial\alpha\partial\beta}\right]v + \left[\mu_1\frac{\partial}{\partial\alpha} + c^2\left(k_2\frac{\partial^3}{\partial\alpha\partial\beta^2} - \frac{\partial^3}{\partial\alpha^3}\right)\right]w = \frac{\rho h R^2[1-(e_o a)^2\nabla^2]}{K}\frac{\partial^2 u}{\partial t^2} \tag{26}$$

$$\left[(\mu_1+k_2)\frac{\partial^2}{\partial\alpha\partial\beta}\right]u + \left[k_2(1+3c^2)\frac{\partial^2}{\partial\alpha^2} + k_1\frac{\partial^2}{\partial\beta^2}\right]v + \left[k_1\frac{\partial}{\partial\beta} - c^2(\mu_1+3k_2)\frac{\partial^3}{\partial\alpha^2\partial\beta}\right]w = \frac{\rho h R^2[1-(e_o a)^2\nabla^2]}{K}\frac{\partial^2 v}{\partial t^2} \tag{27}$$

$$\left[\mu_1\frac{\partial}{\partial\alpha} - c^2\left(\frac{\partial^3}{\partial\alpha^3} - k_2\frac{\partial^3}{\partial\alpha\partial\beta^2}\right)\right]u + \left[k_1\frac{\partial}{\partial\beta} - c^2(\mu_1+3k_2)\frac{\partial^3}{\partial\alpha^2\partial\beta}\right]v + \left[\left(1+\frac{1}{c^2}\right)k_1 + \frac{\partial^4}{\partial\alpha^4} + k_1\frac{\partial^4}{\partial\beta^4} + 2k_1\frac{\partial^2}{\partial\beta^2} + (2\mu_1+4k_2)\frac{\partial^4}{\partial\alpha^2\partial\beta^2}\right]c^2 w + \frac{R^2}{K}(1-(e_0 a)^2\nabla^2)\left[Ew + \eta\frac{\partial w}{\partial t}\right] = -\frac{\rho h R^2[1-(e_o a)^2\nabla^2]}{K}\frac{\partial^2 w}{\partial t^2} \tag{28}$$

where $K = \frac{E_1 h}{1-\mu_1\mu_2}$, medium has stiffness E, and the viscosity of the medium is η. Three kinds of boundary conditions may be assumed while solving such problems (Ansari and Arash 2013). These three conditions are:

Simply supported-simply supported

$$\beta = \gamma = M_{\alpha\alpha} = N_{\alpha\alpha} = 0 \quad \text{at} \quad \alpha = 0, \alpha = L/R \tag{29}$$

Clamped-clamped

$$\alpha = \beta = \gamma = \frac{\partial\gamma}{\partial\alpha} = 0 \quad \text{at} \quad \alpha = 0, \alpha = L/R \tag{30}$$

Clamped-free

$$\begin{cases} \alpha = \beta = \gamma = \frac{\partial\gamma}{\partial\alpha} = 0 \quad \text{at} \quad \alpha = 0 \\ N_{\alpha\alpha} = M_{\alpha\alpha} = N_{\alpha\beta} = M_{\alpha\beta} = 0 \quad \text{at} \quad \alpha = L/R \end{cases} \tag{31}$$

where L is the length of MTs.

Using any combination of above three conditions we come close to nonlocal Flugge's shell model. Above system of equations is the nonlocal orthotropic Kelvin-like shell model for MTs. To understand the waves propagating in MTs, we need to derive the dispersion relations.

2.2 Wave propagation in embedded microtubules

Here, we will discuss wave solutions for axisymmetric and nonaxisymmetric waves.

2.2.1 Axisymmetric waves

The solutions of system of Eqs. (26)-(28) for axisymmetric waves is given by Wang and Gao (2016)

$$\begin{cases} u(\alpha,t) = U e^{ik\left(\alpha - \frac{vt}{R}\right)} \\ v(\alpha,t) = V e^{ik\left(\alpha - \frac{vt}{R}\right)} \\ w(\alpha,t) = W e^{ik\left(\alpha - \frac{vt}{R}\right)} \end{cases} \tag{32}$$

where U, V and W are the amplitudes of waves along the direction of x, y and z respectively, the dimensionless wave vector in the longitudinal direction is $k = \frac{\pi m R}{L}$, in longitudinal direction m is the half axial wave number and v is the wave phase velocity.

Substituting Eq. (32) in system of Eqs. (26)-(28) and simplifying, in matrix form, we get the following system

$$[M^{(1)}(k,v)]_{3\times3}\begin{bmatrix}U\\V\\W\end{bmatrix} = [0 \quad 0 \quad 0]^T \tag{33}$$

For the nontrivial solution of above equation, we have

$$Det[M^{(1)}(k,v)] = 0 \tag{34}$$

2.3 Nonaxisymmetric waves

In case of nonaxisymmetric waves, the solutions of system of Eqs. (28)-(30) and boundary conditions in Eqs. (29)-(31) are given by

$$\begin{cases} u(\alpha,\beta,t) = U e^{ik\left(\alpha - \frac{vt}{R}\right)}.\cos n\beta \\ v(\alpha,\beta,t) = V e^{ik\left(\alpha - \frac{vt}{R}\right)}.\sin n\beta \\ w(\alpha,\beta,t) = W e^{ik\left(\alpha - \frac{vt}{R}\right)}.\cos n\beta \end{cases} \tag{35}$$

where U, V and W are the amplitudes of waves along the direction of x, y and z respectively, in the longitudinal direction, the dimensionless wave vector is $k = \frac{\pi m R}{L}$, in circumferential direction n is the half wave number and v is the wave phase velocity.

Putting Eq. (35) in system of Eqs. (26)-(28) will give us the three homogeneous equations and in matrix form they are given as

$$[M^{(2)}(k,v)]_{3\times3}\begin{bmatrix}U\\V\\W\end{bmatrix} = [0 \quad 0 \quad 0]^T \tag{36}$$

The nonzero solution of above system exists if

Table 1 Comparison of nondimensional frequencies $\Delta = \omega R\sqrt{\rho/E}$ (L/R = 1, n = 1)

m	n = 1		n = 2	
	Alibeigloo and Shaban (2013)	Present	Alibeigloo and Shaban (2013)	Present
0	0.97087	0.97063	0.99351	0.99289
1	0.59721	0.59698	0.88357	0.88301
2	0.34025	0.34019	0.68072	0.68013
3	0.20145	0.20099	0.50059	0.5003
4	0.12886	0.12872	0.36918	0.36897
5	0.09105	0.9087	0.27671	0.27662

Table 2 Comparison of the nondimentionalized WPA natural frequencies parameters $\Delta = \omega R\sqrt{\frac{\rho[1-\upsilon]}{E}}$ of SWCNT (υ = 0.3, h/R = 0.01)

L/R	Method	m					
		0	1	2	3	4	5
0.5	Liew (2005)	0.8732	0.812	0.6696	0.5428	0.4565	0.4088
	Heydarpour *et al*. (2014)	0.8725	0.8116	0.6694	0.5426	0.4563	0.4088
	Present	0.8732	0.812	0.6696	0.5428	0.4565	0.4088

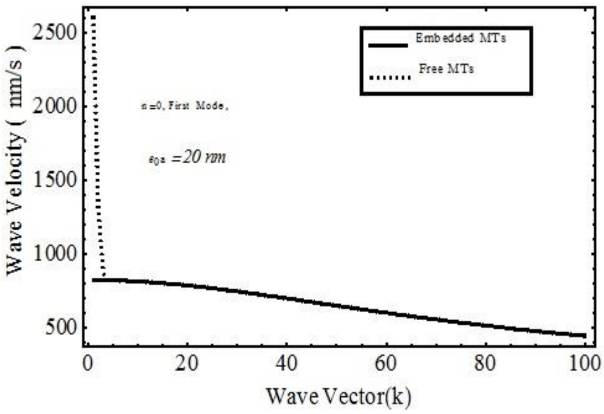

Fig. 2 Effects of viscoelastic medium (modeled by Kelvin model) on the speed of axisymmetric waves of the first mode

$$Det\left[M^{(2)}(k,\upsilon)\right] = 0 \tag{37}$$

3. Results

We are studying nonlocal behavior of MTs. Comparisons of embedded and free MTs are made for axisymmetric and nonaxisymmetric waves of each mode separately. At the end, the combined graphs of all modes are discussed for axisymmetric and nonaxisymmetric waves. Since the percentage of error is negligible, the model is concluded as valid. An innovative technique for the

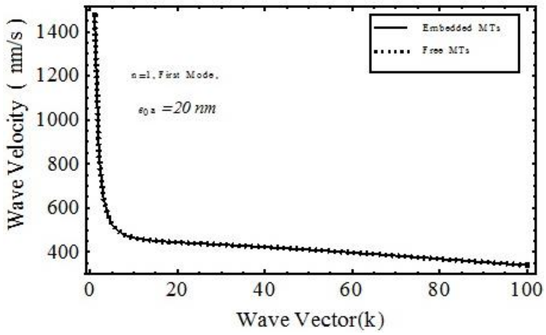

Fig. 3 Comparison between wave speeds of non-axisymmetric waves of the first mode for free and embedded MTs

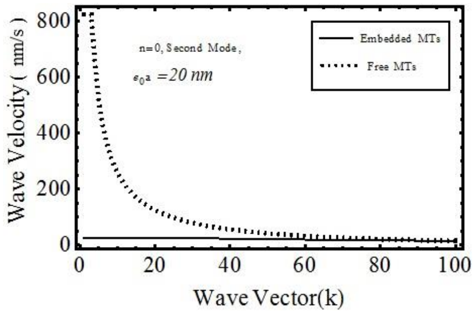

Fig. 4 Effects of viscoelastic medium (modeled by Kelvin model) on the speed of axisymmetric waves of the second mode

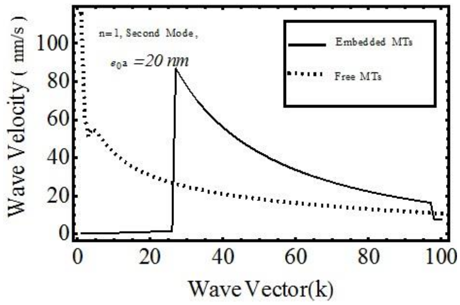

Fig. 5 Comparison between wave speeds of non-axisymmetric waves of the second mode for free and embedded MTs

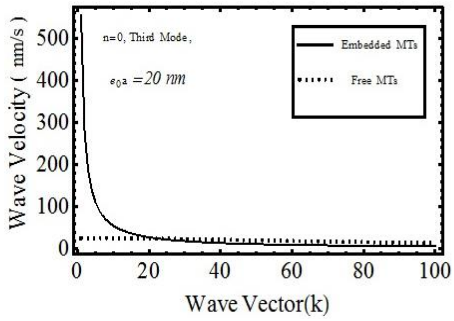

Fig. 6 Effects of viscoelastic medium (modeled by Kelvin model) on the speed of axisymmetric waves of the third mode

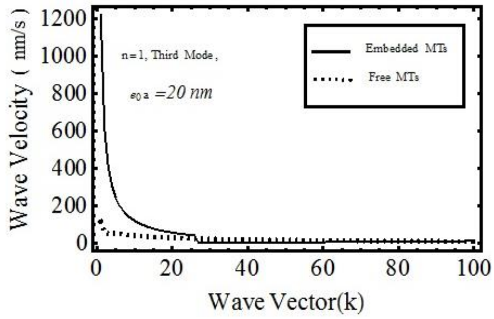

Fig. 7 Comparison between wave speeds of non-axisymmetric waves of the third mode for free and embedded MTs

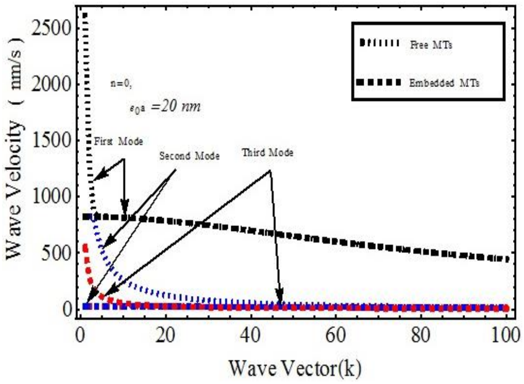

Fig. 8 Effect of viscoelastic medium (modeled by Kelvin model) on the speeds of axisymmetric waves produced in MTs

behavior of embedded MTs with the effect of nonlocal parameter is investigated. The structural parameters are used here taken from Ref. (Wang and Gao 2016, Safeer *et al*. 2019). A comparison of nondimensionalized natural frequencies $\Delta = \omega R\sqrt{\rho/E}$ of SWCNT is presented in Table 1. It is noted that from Table 1, the frequency value of present model has the small values as the values followed by the Alibeigloo and Shaban (2013) shows a frequency difference between these studies. It can be seen that the error percentage is negligible, hence showing high rate of convergence. The results of nondimensional frequency are computed for two different values of n = 1, 2 with circumferential wave number (m = 0, 1, 2, 3, 4, 5) as shown in Table 1. Alibeigloo and Shaban (2013) investigated the impact of nonlocal parameters on the vibration of CNTs by using the three-dimensional elastic theory based on the Fourier series expansion. A comparison of non-dimensionalized natural frequencies presents in Table 2 and the natural frequencies of Table 2 based on Kelvin's model are compared with different researchers (Liew 2005, Heydarpour *et al*. 2014). From the above comparisons of frequencies, it is noticed that there is a good coincidence between these results and other ones calculated by different numerical techniques. Hence it is concluded that the analytical procedure applied here is valid and efficient and gives accurate results. It can be adopted to analyze vibrations of the present nanotube problem.

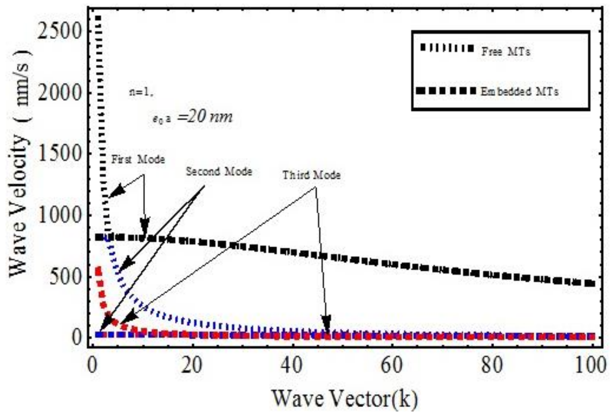

Fig. 9 Effect of viscoelastic medium (modeled by Kelvin model) on the speeds of nonaxisymmetric waves produced in MTs

The proposed model based on Kelvin's model can incorporate in order to accurately predict the acquired results of material data point. Fig. 2 demonstrates the effects of viscoelastic medium around MTs on speed of axisymmetric waves of the first mode produced in MTs. The wave velocity is plotted against the wave vector k. In the figure given below, comparison of velocities for free and embedded MTs is made for nonlocal theory taking e_0a = 20 nm. For very small values of k, the speed of free MTs starts decreasing from 2620 nms^{-1}. This fall is very sharp until k reaches to 3 and velocity becomes 823 nms^{-1} and then decreases smoothly. By taking the natural viscoelastic medium of MTs in account, it is seen that the maximum value of wave speed is reduced up to 827 nms^{-1}. At k = 3 the wave speeds are same for embedded and free MTs and speed reduces in the same manner. Physically these results are very close to natural process of reduction in speed due to presence of medium. There is no difference in the speeds except for k < 3. Fig. 3 explains the effects of medium for nonaxisymmetric waves of the first mode by taking e_0a = 20 nm which discusses the nonlocal theory. Fig. 3 shows that there is no change in speed of waves of the second kind due to the presence of medium. In Fig. 4, relationship between speed of axisymmetric wave and wave vector is explained graphically for the waves of the second mode by considering non local effects. The effect of surrounding medium for the speed of axisymmetric waves of the second mode is debated. In case of free MTs, the maximum speed of waves is much greater than the embedded MTs. The value of maximum speed decreases from 827 nms^{-1} to 26 nms^{-1} by consideration of the medium. For very large values of k, velocity in both of the cases tends to zero. Speed of waves for free MTs fall abruptly for small values of k and with the growth of k, this decrease in velocity becomes gradually slow. This figure explains the natural effects of actual surrounding medium on the velocity of waves. Fig. 5 corresponds to the effects of surrounding medium for nonaxisymmetric waves of the second mode. For very small values of k, the speed of waves in free MTs is 117 nms^{-1} and continue to decrease with the growth of k while for embedded MTs the speed of wave is zero and increases suddenly up to 86 nms^{-1} at k = 26 and then continuously decrease down for larger values of k. Fig. 6 relates the effects of surrounding medium for axisymmetric waves of the third mode. The behavior seen in this case is contrary to that of Fig. 4. Therefore, one can conclude that the axisymmetric wave of second mode for free MTs behave like axisymmetric wave of third mode for embedded MTs and vice versa. In Fig. 7, the effects of viscoelastic medium for nonaxisymmetric waves of the third mode are deliberated. The conclusion is also contrary to that of the case of second mode nonaxisymmetric waves. Wave of second mode for embedded MTs in Fig. 5 resembles the wave of free MTs of this case. Also, wave of second mode for free MTs in Fig. 5 resembles the wave of embedded MTs of this case. The behaviors are interchanged due to consideration of viscoelastic medium. Fig. 8 symbolizes the effects of medium for axisymmetric waves. This figure ensures the decrease in speeds due to medium. Here, due to presence of surrounding medium in the first mode, the maximum speed decreases from 2620 nms^{-1} to 827 nms^{-1} and for $k > 3$ the curves coincide. It is observed that the curve for the third mode of free MTs is same as the curve of second mode of embedded MTs. In both of the cases the maximum speed is 26 nms^{-1} and with the growth of k it tends to zero. The curves for the second mode of free MTs and the curve of third mode for embedded MTs are similar in shape. However, both the curves have different routes for $k < 55$. The maximum speed for wave of second mode in free MTs is 827 nms^{-1} and for embedded MTs bearing wave of third mode is 564 nms^{-1}. Therefore, it is seen that the speed of waves change remarkably because the surrounding medium exerts external pressure on the outer surface of MTs, so the speed of waves is altered. In Fig. 9, we have plots that represent the change in mode or speed due to viscoelastic medium for nonaxisymmetric waves. There is no change in first mode because these waves are longitudinal waves and medium is exerting pressure in radial direction only. The curves for second and third modes of waves in free MTs are same and the maximum value of velocity is 117 nms^{-1}.

4. Perspectives and conclusions

The current study presented the viscoelastic medium along with nonlocal elastic theory. The analytical formulas of the velocity of waves, and the results reveal that the presence of medium reduces the velocity. The axisymmetric and nonaxisymmetric waves have separately discussed. Moreover, the results are compared with the results gained from the studies of free microtubules. The effects of viscoelastic medium, nonaxisymmetric waves for first mode and relationship between speed of axisymmetric wave and wave vector, nonaxisymmetric waves for second and 3rd mode have been discussed in detail. The analysis done with the findings

• Microtubules, though very small in size, perform a vital role in transportation of protein and in maintaining the cell shape. During performing these functions waves propagate and this propagation of waves has been investigated using nonlocal elastic theory.

• The presence of medium around microtubules results in the increase of the flexural rigidity causing a significant decrease in radial wave velocity as compared to axial and circumferential wave velocities.

• The effect of viscoelastic medium is more obvious on radial wave velocity, to a lesser extent on torsional wave velocity and least on longitudinal wave velocity.

• For the case of axisymmetric wave and wave vector the maximum speed of waves is much greater than the embedded MTs. The value of maximum speed decreases from 827 nms^{-1} to 26 nms^{-1} by consideration of the medium.

• Therefore, one can conclude that the axisymmetric wave of second mode for free MTs behave like axisymmetric wave of third mode for embedded MTs and vice versa.

• The conclusion is also contrary to that of the case of second mode nonaxisymmetric waves. Wave of second mode for embedded MTs. The behaviours are interchanged due to consideration of viscoelastic medium.

• Therefore, it is seen that the speed of waves change remarkably because the surrounding medium exerts external pressure on the outer surface of MTs, so the speed of waves is altered.

The present study can be appropriate to employ for analyzing the kelvin's model with embedded microtubules using finite element method.

Declaration of conflicting interests

The author(s) declared no potential conflicts of interest with respect to the research, authorship, and/or publication of this article.

Acknowledgments

The research team thanks the efforts of King Khalid University in financing this applied research and providing all the facilities (laboratories, hardware and software) in the College of Engineering. In addition, special thanks to Civil Engineering Department where this applied research work achieved. Finally, thanks again to Deanship of Scientific Research in King Khalid University to continue to support scientific research until it becomes among the best universities locally and internationally. Within the framework of small research projects given by the Deanship of Scientific Research the grant number is 305.

References

Alibeigloo, A. and Shaban, M. (2013), "Free vibration analysis of carbon nanotubes by using three-dimensional theory of elasticity", *Acta Mech*., **224**, 1415-1427. https://doi.org/10.1007/s00707-013-0817-2.

AlSaleh, R.J. and Fuggini, C. (2020), "Combining GPS and accelerometers' records to capture torsional response of cylindrical tower", *Smart Struct. Syst., Int. J.*, **25**(1), 111-122. https://doi.org/10.12989/sss.2020.25.1.111.

An, L. and Gao, Y. (2010), "Mechanics behavior of microtubules

based on nonlocal anisotropic shell theory", *IOP Confer. Series Mater. Sci. Eng.*, **10**(1), 012181. https://doi.org/10.1088/1757-899X/10/1/012181.
Ansari, R. and Arash, B. (2013), "Nonlocal Flügge shell model for vibrations of double-walled carbon nanotubes with different boundary conditions", *J. Appl. Mech.*, **80**(2), 021006. https://doi.org/80/2/021006/370643.
Arani, A.G., Kolahchi, R. and Esmailpour, M. (2016), "Nonlinear vibration analysis of piezoelectric plates reinforced with carbon nanotubes using DQM", *Smart Struct. Syst., Int. J.*, **18**(4), 787-800. http://dx.doi.org/10.12989/sss.2016.18.4.787.
Arefi, M. and Zenkour, A.M. (2017), "Nonlinear and linear thermo-elastic analyses of a functionally graded spherical shell using the Lagrange strain tensor", *Smart Struct. Syst., Int. J.*, **19**(1), 33-38. https://doi.org/10.12989/sss.2017.19.1.033.
Arefi, M., Mohammadi, M., Tabatabaeian, A., Dimitri, R. and Tornabene, F. (2018), "Two-dimensional thermo-elastic analysis of FG-CNTRC cylindrical pressure vessels", *Steel Compos. Struct., Int. J.*, **27**(4), 525-536. https://doi.org/10.12989/scs.2018.27.4.525.
Born, M. and Huang, K. (1954), *Dynamical Theory of Crystal Lattices*, Clarendon press, London, UK.
Boussoula, A., Boucham, B., Bourada, M., Bourada, F., Tounsi, A., Bousahla, A.A. and Tounsi, A. (2019), "A simple nth-order shear deformation theory for thermomechanical bending analysis of different configurations of FG sandwich plates", *Smart Struct. Syst., Int. J.*, **25**(2), 197-218. https://doi.org/10.12989/sss.2020.25.2.197.
Boutaleb, S., Benrahou K.H., Bakora, A., Algarni, A., Bousahla, A.A., Tounsi, A. and Mahmoud, S.R. (2019), "Dynamic analysis of nanosize FG rectangular plates based on simple nonlocal quasi 3D HSDT", *Adv. Nano Res., Int. J.*, **7**(3), 189-206. https://doi.org/10.12989/anr.2019.7.3.189.
Civalek, Ö. and Demir, Ç. (2011), "Bending analysis of microtubules using nonlocal Euler-Bernoulli beam theory", *Appl. Math. Model.*, **35**(5), 2053-2067. https://doi.org/10.1016/j.apm.2010.11.004.
Civalek, Ö., Demir, Ç. and Akgöz, B. (2010), "Free vibration and bending analyses of cantilever microtubules based on nonlocal continuum model", *Math. Comput. Appl.*, **15**(2), 289-298. https://doi.org/10.3390/mca15020289.
Daneshmand, F., Ghavanloo, E. and Amabili, M. (2011), "Wave propagation in protein microtubules modeled as orthotropic elastic shells including transverse shear deformations", *J. Biomech.*, **44**(10), 1960-1966. https://doi.org/10.1016/j.jbiomech.2011.05.003.
De Pablo, P.J., Schaap, I.A., MacKintosh, F.C. and Schmidt, C.F. (2003), "Deformation and collapse of microtubules on the nanometer scale", *Phys. Rev. Lett.*, **91**(9), 098101. https://doi.org/0.1103/PhysRevLett.91.098101.
Do, Q.C., Pham, D.N., Vu, D.Q., Vu, T.T.A. and Nguyen, D.D. (2019), "Nonlinear buckling and post-buckling of functionally graded CNTs reinforced composite truncated conical shells subjected to axial load", *Steel Compos. Struct., Int. J.*, **31**(3), 243-259. https://doi.org/10.12989/scs.2019.31.3.243.
Eringen, A.C. (1972), "Linear theory of nonlocal elasticity and dispersion of plane waves", *Int. J. Eng. Sci.*, **10**(5), 425-435. https://doi.org/10.1016/0020-7225(72)90050-X.
Eringen, A.C. (1977), "Relation between non-local elasticity and lattice dynamics", *Crystal Latt. Def.*, **7**, 51-57. https://ci.nii.ac.jp/naid/80014851754.
Eringen, A.C. (2002), *Nonlocal Continuum Field Theories*, Springer Science & Business Media, Colorado, USA.
Flugge, S., (1973), *Stresses in Shells*, Springer, Berlin, Germany.
Gao, Y. and Lei, F.M. (2009), "Small scale effects on the mechanical behaviors of protein microtubules based on the nonlocal elasticity theory", *Biochem. Biophys. Res. Commun.*, **387**(3), 467-471. https://doi.org/10.1016/j.bbrc.2009.07.042.
Gao, Y. and An, L. (2010), "A nonlocal elastic anisotropic shell model for microtubule buckling behaviors in cytoplasm", *Physica E Low Dimens. Syst. Nanostruct.*, **42**(9), 2406-2415. https://doi.org/10.1016/j.physe.2010.05.022.
Gittes, F., Mickey, B., Nettleton, J. and Howard, J. (1993), "Flexural rigidity of microtubules and actin filaments measured from thermal fluctuations in shape", *J. Cell Biol.*, **120**(4), 923-934. http://doi.org/10.1083/jcb.120.4.923.
Heydarpour, Y., Aghdam, M. and Malekzadeh, P. (2014), "Free vibration analysis of rotating functionally graded carbon nanotube-reinforced composite truncated conical shells", *Compos. Struct.*, **117**, 187-200. http://doi.org/10.1016/j.compstruct.2014.06.023.
Hussain, M. and Naeem, M.N. (2019a), "Rotating response on the vibrations of functionally graded zigzag and chiral single walled carbon nanotubes", *Appl. Math. Model*, **75**, 506-520. https://doi.org/10.1016/j.apm.2019.05.039.
Hussain, M. and Naeem, M.N. (2019b), "Effects of ring supports on vibration of armchair and zigzag FGM rotating carbon nanotubes using Galerkin's method", *Compos. Part B Eng.*, **163**, 548-561. https://doi.org/10.1016/j.compositesb.2018.12.144.
Hussain, M., Naeem. M., Tounsi, A. and Taj, M. (2019), "Nonlocal effect on the vibration of armchair and zigzag SWCNTs with bending rigidity", *Adv. Nano Res., Int., J.*, **7**(6), 431-442. https://doi.org/10.12989/anr.2019.7.6.431.
Ishida, T., Thitamadee, S. and Hashimoto, T. (2007), "Twisted growth and organization of cortical microtubules", *J. Plant Res.*, **120**(1), 61-70. https://doi.org/10.1007/s10265-006-0039-y.
Kasas, S., Cibert, C., Kis, A., De Rios, P.L., Riederer, B.M., Forro, L., Dietler, G. and Catsicas, S. (2004), "Oscillation modes of microtubules", *Biol. Cell*, **96**(9), 697-700. https://doi.org/10.1016/j.biolcel.2004.09.002.
Krommer, M., Vetyukova, Y. and Staudigl, E. (2016), "Nonlinear modelling and analysis of thin piezoelectric plates: Buckling and post-buckling behavior", *Smart Struct. Syst., Int. J.*, **18**(1), 155-181. https://doi.org/10.12989/sss.2016.18.1.155.
Kröner, E. (1967), "Elasticity theory of materials with long range cohesive forces", *Int. J. Solids Struct.*, **3**(5), 731-742. https://doi.org/10.1016/0020-7683(67)90049-2.
Lee, S.Y., Huynh, T.C., Dang, N.L. and Kim, J.T. (2019), "Vibration characteristics of caisson breakwater for various waves, sea levels, and foundations", *Smart Struct. Syst., Int. J.*, **24**(4), 525-539. https://doi.org/10.12989/sss.2019.24.4.525.
Lei, Z. and Zhang, Y. (2018), "Characterizing buckling behavior of matrix-cracked hybrid plates containing CNTR-FG layers", *Steel Compos. Struct., Int. J.*, **28**(4), 495-508. https://doi.org/10.12989/scs.2018.28.4.495.
Li, C., Ru, C.Q. and Mioduchowski, A. (2006), "Length-dependence of flexural rigidity as a result of anisotropic elastic properties of microtubules", *Biochem. Biophys. Res. Commun.*, **349**(3), 1145-1150. https://doi.org/10.1016/j.bbrc.2006.08.153.
Liew, K.M., Ng, T.Y. and Zhao, X. (2005), "Free vibration analysis of conical shells via the element-free kp-Ritz method", *J Sound Vib.*, **281**, 627-645. https://doi.org/10.1016/j.jsv.2004.01.005.
Moradi-Dastjerdi, R. and Payganeh, G. (2017), "Transient heat transfer analysis of functionally graded CNT reinforced cylinders with various boundary conditions", *Steel Compos. Struct., Int. J.*, **24**, 359-367. https://doi.org/10.12989/scs.2017.24.3.359.
Needleman, D.J., Ojeda-Lopez, M.A., Raviv, U., Ewert, K., Miller, H.P., Wilson, L. and Safinya, C.R. (2005), "Radial compression of microtubules and the mechanism of action of taxol and associated proteins", *Biophys. J.*, **89**(5), 3410-3423.

https://doi.org/10.1529/biophysj.104.057679.
Nogales, E. (2001), "Structural insights into microtubule function", *Ann. Rev. Biophys. Biomol. Struct.*, **30**(1), 397-420. https://doi.org/10.1146/annurev.biophys.30.1.397.
Paliwal, D.N., Kanagasabapathy, H. and Gupta, K.M. (1995), "The large deflection of an orthotropic cylindrical shell on a Pasternak foundation", *Compos. Struct.*, **31**(1), 31-37. https://doi.org/10.1016/0263-8223(94)00068-9.
Poplawski, B., Mikulowski, G., Pisarski, D., Wiszowaty, R. and Jankowski, L. (2019), "Optimum actuator placement for damping of vibrations using the prestress-accumulation release control approach", *Smart Struct. Syst., Int. J.*, **24**(1), 27-35. https://doi.org/10.12989/sss.2019.24.1.027.
Qian, X.S., Zhang, J.Q. and Ru, C.Q. (2007), "Wave propagation in orthotropic microtubules", *J. Appl. Phys.*, **101**(8), 084702. https://doi.org/10.1063/1.2717573.
Safeer, M., Taj, M. and Abbas, S.S. (2019), "Effect of viscoelastic medium on wave propagation along protein microtubules", *AIP Adv.*, **9**(4), 045108. https://doi.org/10.1063/1.5086216.
Shafiei, H. and Setoodeh, A.R. (2017), "Nonlinear free vibration and post-buckling of FG-CNTRC beams on nonlinear foundation", *Steel Compos. Struct., Int. J.*, **24**(1), 65-77. https://doi.org/10.12989/scs.2017.24.1.065.
She, G.L., Ren, Y.R. and Yuan, F.G. (2019), "Hygro-thermal wave propagation in functionally graded double-layered nanotubes systems", *Steel Compos. Struct., Int. J.*, **31**(6), 641-653. https://doi.org/10.12989/scs.2019.31.6.641.
Shen, H.S. (2010a), "Nonlocal shear deformable shell model for postbuckling of axially compressed microtubules embedded in an elastic medium", *Biomech. Model. Mechanobiol.*, **9**(3), 345-357. https://doi.org/10.1007/s10237-009-0180-3.
Shen, H.S. (2010b), "Buckling and postbuckling of radially loaded microtubules by nonlocal shear deformable shell model", *J. Theor. Biol.*, **264**(2), 386-394. https://doi.org/10.1016/j.jtbi.2010.02.014.
Shen, H.S. (2011), "Nonlinear vibration of microtubules in living cells", *Curr. Appl. Phys.*, **11**(3), 812-821. https://doi.org/10.1016/j.cap.2010.11.116.
Tahouneh, V. (2017), "Effects of CNTs waviness and aspect ratio on vibrational response of FG-sector plate", *Steel Compos. Struct., Int. J.*, **25**(6), 649-661. https://doi.org/10.12989/scs.2017.25.6.649.
Taj, M. and Zhang, J.Q. (2011), "Buckling of embedded microtubules in elastic medium", *Appl. Math. Mech.*, **32**(3), 293-300. https://doi.org/10.1007/s10483-011-1415-x.
Taj, M. and Zhang, J.Q. (2012), "Analysis of vibrational behaviors of microtubules embedded within elastic medium by Pasternak model", *Biochem. Biophys. Res. Commun.*, **424**(1), 89-93. https://doi.org/10.1016/j.bbrc.2012.06.072.
Taj, M. and Zhang, J. (2014), "Analysis of wave propagation in orthotropic microtubules embedded within elastic medium by Pasternak model", *J. Mech. Behav. Biomed. Mater.*, **30**, 300-305. https://doi.org/10.1016/j.jmbbm.2013.11.011.
Tohidi, H., Hosseini-Hashemi, S.H. and Maghsoudpour, A. (2018), "Size-dependent forced vibration response of embedded micro cylindrical shells reinforced with agglomerated CNTs using strain gradient theory", *Smart Struct. Syst., Int. J.*, **22**(5), 527-546. https://doi.org/10.12989/sss.2018.22.5.527.
Tuszyński, J.A., Luchko, T., Portet, S. and Dixon, J.M. (2005), "Anisotropic elastic properties of microtubules", *Eur. Phys. J. E*, **17**(1), 29-35. https://doi.org/10.1140/epje/i2004-10102-5.
Wang, C.Y., Ru, C.Q. and Mioduchowski, A. (2006), "Orthotropic elastic shell model for buckling of microtubules", *Phys. Rev. E*, **74**(5), 052901. https://doi.org/10.1103/PhysRevE.74.052901.
Wang, J. and Gao, Y. (2016), "Nonlocal orthotropic shell model applied on wave propagation in microtubules", *Appl. Math. Model.*, **40**(11-12), 5731-5744. https://doi.org/10.1016/j.apm.2016.01.013.
Wang, Q. and Varadan, V.K. (2007), "Application of nonlocal elastic shell theory in wave propagation analysis of carbon nanotubes", *Smart Mater. Struct.*, **16**(1), 178. https://doi.org/10.1088/0964-1726/16/1/022.
Yeh, J.Y. (2016), "Vibration characteristic analysis of sandwich cylindrical shells with MR elastomer", *Smart Struct. Syst., Int. J.*, **18**(2), 233-247. https://doi.org/10.12989/sss.2016.18.2.233
Zahrai, S.M. and Kakouei, S. (2019), "Shaking table tests on a SDOF structure with cylindrical and rectangular TLDs having rotatable baffles", *Smart Struct. Syst., Int. J.*, **24**(3), 391-401. https://doi.org/10.12989/sss.2019.24.3.391.
Zou, R.D. and Foster, C.G. (1995), "Simple solution for buckling of orthotropic circular cylindrical shells", *Thin-Wall. Struct.*, **22**(3), 143-158. https://doi.org/10.1016/0263-8231(94)00026-V.

FC